

2

EFFECTS OF HIGH THERMAL AND HIGH FAST FLUENCES ON THE
MECHANICAL PROPERTIES OF TYPE 6061 ALUMINUM IN THE HFBR*

John R. Weeks and Carl J. Czajkowski

BNL--42692

Department of Nuclear Energy

DE89 012636

and

Paul R. Tichler

Reactor Division

Brookhaven National Laboratory

Upton, New York 11973

Received by OSTI

JUN 06 1989

ABSTRACT

The High Flux Beam Reactor (HFBR) at Brookhaven National Laboratory (BNL) is an epithermal, externally moderated (by D₂O) facility designed to produce neutron beams for research. Type 6061 T-6 aluminum was used for the beam tubes, pressure vessel, fuel cladding, and most other components in the high flux area. The HFBR has operated since 1965.

The epithermal, external moderation of the HFBR means that materials irradiated in different areas of the facility receive widely different flux spectra. Thus, specimens from a control rod drive follower tube (CRDF) have received $1.5 \times 10^{22} \text{n/cm}^2$ (E>0.1MeV) and $3.2 \times 10^{23} \text{n/cm}^2$ thermal fluence, while those from a vertical thimble flow shroud received $1.9 \times 10^{23} \text{n/cm}^2$ (E>0.1MeV) and $1.0 \times 10^{23} \text{n/cm}^2$ thermal. These numbers correspond to fast to thermal

*Work performed under the auspices of the U.S. Department of Energy, Office of Basic Energy Sciences.

DISCLAIMER

This report was prepared as an account of work sponsored by an agency of the United States Government. Neither the United States Government nor any agency thereof, nor any of their employees, makes any warranty, express or implied, or assumes any legal liability or responsibility for the accuracy, completeness, or usefulness of any information, apparatus, product, or process disclosed, or represents that its use would not infringe privately owned rights. Reference herein to any specific commercial product, process, or service by trade name, trademark, manufacturer, or otherwise does not necessarily constitute or imply its endorsement, recommendation, or favoring by the United States Government or any agency thereof. The views and opinions of authors expressed herein do not necessarily state or reflect those of the United States Government or any agency thereof.

MASTER

Sx

fluence ratios ranging from 0.05 to 1.9. Irradiations are occurring at approximately 333°K. The data indicate that the increase in tensile strength and decrease in ductility result primarily from the thermal fluence, i.e., the transmutation of aluminum to silicon. These effects appear to be saturating at fluences above approximately $1.8 \times 10^{23} \text{n/cm}^2$ thermal at values of 90,000 psi (6700 Kg/mm^2) and 9%, respectively. The specimens receiving the highest fluence ratios appear to have less increase in tensile strength and less decrease in ductility than specimens with a lower fast to thermal fluence ratio and the same thermal fluence, suggesting a possible beneficial effect of the high energy neutrons in preventing formation of silicon crystallites.

KEY WORDS: Radiation, Aluminum Alloys, Thermal Fluence Effect, High Flux
Research Reactors

INTRODUCTION

The High Flux Beam Reactor (HFBR) is a heavy water-cooled and moderated reactor. The core is undermoderated, with most of the moderating occurring in the reflector. It was specifically designed to produce high intensity beams of neutrons of various energies for research purposes. The entire vessel, including the re-entrant beam tubes, is one welded structure made of type 6061 aluminum heat treated after welding to the T-6 condition. Criticality was first achieved on October 31, 1965; the original design life was for 20 years of operation at 40 MWth. In 1980 the core loading was increased and new heat exchangers installed to permit operating at 60 MWth.

Since the research programs that use the facility are anticipated to continue, BNL is attempting to extend the useful life of the facility for as long as possible. The purpose of this paper is to describe what is known about the effects of long term exposure to the reactor environment, especially radiation, on the vessel material, type 6061 aluminum.

Figure 1 shows a cutaway of the reactor vessel, giving the relative position of the horizontal ("H") and vertical ("V") beam tubes with respect to the core. Figure 2 shows the flux profile for 60 MW operation⁽¹⁾. As can be seen, the fast neutron flux (curves 1 & 2) peaks in the core region whereas the thermal neutron flux (curve 7) peaks in the reflector region. Thus, in the extreme cases, the fast to thermal flux ratio varies from ~5 in the central core to <0.05 in the peak thermal flux region. The beam tubes were designed to provide neutron beams of varying spectra for neutron physics research.

When the reactor was designed, a series of capsules containing coupons was placed in the vertical core-edge thimble, V-13. An early concern was radiation-induced overaging by γ -heating of the beam tube tips, so an attempt was made to irradiate these specimens over a range of temperatures. However, subsequent measurements of the temperatures of the beam tube tips showed γ -heating to be negligible, so all subsequent coupon irradiations have been performed at reactor core outlet ambient temperature, (333°K). Early in the cycle, several sets of coupons were examined, and fresh ones inserted in their place. The coolant/moderator is high purity D_2O , acidified to pH 5.0-5.2 with nitric acid. In addition to these specimens, a vertical thimble flow shroud (from V-15) and 3 control rod follower tubes, all fabricated of 6061 T-6, have been removed and examined.

Since the purpose of the surveillance program is to monitor the effects of irradiation on the beam tube tips, let us compare the approximate doses on these specimens with the doses on the highest exposure beam tube tip - "H-2": The capsule surveillance specimens lead the H-2 tip by ~3x in fast ($E > 1\text{MeV}$) neutrons, but lag it by about 3x in thermal neutrons. The V-15 flow shroud sees a wide range of fast to thermal fluence ratios as it extends from the central core region up through the peak thermal flux region above the core. The control rod drive followers, being external to the core, see essentially the same thermal flux as the H-2 tip with a slightly higher fast flux background.

At the time the HFBR was being designed (1962-1963), the belief was that fast neutrons are the principal cause of radiation damage to the material. Further, since 6061 T-6 is a fully age-hardened alloy, it contains a massive network of internal sub-critical nuclei (of Mg_2Si) so that little additional strengthening and loss in ductility were anticipated to be caused by fast

neutrons. The available Engineering Test Reactor (ETR) data showed this alloy in this heat treated condition to be essentially unaffected by fast ($E>1\text{MeV}$) fluences up to $1.2 \times 10^{21}\text{n/cm}^2$.⁽²⁾

Farrell et al., (3,4,5) have studied the effects of irradiation on 6061 T-6 in the High Flux Isotope Reactor (HFIR). Their results show that, at a fast to thermal flux ratio of 0.6, a gradual increase in tensile strength and loss in ductility begins at a fast ($E>0.1\text{MeV}$) fluence of 10^{21}n/cm^2 , but that the ductility loss appears to saturate above a fast fluence of 10^{22}n/cm^2 . These results are shown in Figure 3, and led the H-2 beam tube tip in fast fluence at least up to 1985.

As part of the life extension program, all available HFBR surveillance data were compared with the results of Farrell et al; the results were, to us, surprising.

Experimental Methods and Results

Table 1 lists the samples removed from the HFBR together with the fast and thermal fluences as estimated from curves of the type shown in Figure 2. The surveillance coupons are standard machined tensile specimens which were pulled on a MTS tester in the BNL Metallurgy Hot Cell. The CRDF's and the flow shroud, however, are in the form of thin-walled tubing. Figures 4 and 5 show how specimens were cut from these; they were pulled as cut (without flattening) in the MTS tester at a rate of $10^{-5}/\text{sec}$. The results from all surveillance specimens are listed in Table 1. Note that the tensile strength and % elongation for the wrought bar material (from which the surveillance coupons were cut) closely approximate the properties given in the ALCOA Handbook (of 1959 - the date design work got underway) whereas the unirradiated tubing specimens used as standards for CRDF A-6 (examined at Oak Ridge National Laboratory) and A-8 averaged only 10-11% elongation.

Figures 6 and 7 show the HFBR data on tensile strength and % elongation as a function of fast ($E > 0.62$ MeV) fluence. Note, the high fast fluence end of the flow shroud had a low thermal background, and vice-versa (see Table 1), and the specimen from the high fast (low thermal) fluence end shows little effect of irradiation. The apparent peak in tensile strength and minimum in % elongation at intermediate fast fluences, shown in Figures 6 and 7, represent specimens with the lowest fast to thermal fluence ratio, and suggest that the thermal, rather than the fast fluence may have the major effect on these mechanical properties. Figures 8 and 9 show the same data plotted as a function of thermal fluence. These plots show at more "regular" behavior; they also suggest that effects may be "saturating" at a tensile strength of approximately 90 ksi (6700 Kg/mm²) and a total elongation of approximately $9 \pm 2.2\%$. Apparently, the thermal neutron effects of transmutation of Al to Si are greater than the fast neutron effects of atomic displacement in this alloy. Since a fully age-hardened (T-6) alloy already contains a network of defects associated with the Mg₂ Si nuclei, this may not be surprising.

DISCUSSION

Figures 10 and 11 compare the results from the HFBR surveillance with those from Farrell et al⁽⁴⁾ on 6061-Al and those from the Netherland's Petten reactor⁽⁶⁾ (Type 5154 Al), plotted against thermal fluence. The HFIR results, which have a constant $\emptyset_{\text{fast}}/\emptyset_{\text{thermal}}$ of 0.6, show less of an increase than the HFBR CRDF data, obtained with a $\emptyset_{\text{fast}}/\emptyset_{\text{thermal}}$ of 0.05, but more of an increase, at a given \emptyset_{th} , than the data from the V-15 flow shroud, especially those obtained from the in-core end, where $\emptyset_{\text{fast}}/\emptyset_{\text{thermal}}$ was ~2. The Petten data suggest that an alloy higher in Mg than 6061 appears to be increasing in strength and losing ductility more rapidly than 6061 at the same thermal

fluence, presumably by reaction of the radiogenic Si with the Mg to form the stable phase, Mg_2Si . Both in HFBR and in HFIR, the ductility of 6061 appears to reach a minimum value of approximately 9%, and that "saturation" ductility level is probably the most heartening conclusion from this study.

But the question for life-extension considerations is, how much further can these data be extrapolated? Farrell et al^(4,5) identified the silicon as building up at the surfaces of internal voids in the alloy, and found no evidence for crystalline silicon, suggesting that Si buildup could continue well above their maximum of 7% without creation of a grain boundary network of a brittle phase. Alloy 6061 contains only approximately 1% Mg, most of which has already reacted with the Si during the age-hardening process, so the development of a brittle Mg_2Si grain boundary phase, as may have developed in 5154 Al at Petten, is not likely in 6061; the apparent "saturation" ductility value in 6061, but not in 5154 (see Fig. 11), can possibly be explained by this hypothesis. Unfortunately, extrapolation, updated by periodic inservice surveillance (by removing one of the 5 remaining original CRDF's) is about all we can do at the present, since we know of no irradiation facility with thermal fluxes sufficient higher than those in HFBR in which samples could be irradiated to achieve higher fluences than those already received by the HFBR beam tube tips. The absence of any embrittling second phase developing in the HFIR tests is, however, encouraging that further extrapolations to the eutectic composition (12.2 a/o) and even beyond can probably be made without serious problems developing. Extending the life to approximately 40 years ($8.5 \times 10^{23} n/cm^2$, or 16% Si in the H-2 tip) should be, in principle, possible under this argument.

To verify the calculated thermal fluences used in the figures presented above, the specimens used in the V-15 and CRDF A-8 tests were analyzed for silicon wet chemically. The results are given in Tables 2 and 3. In general, the results are in reasonably good agreement with the calculated fluences, especially for the CRDF A-8, the specimens with the highest thermal fluence.

The results from the CRDF A-7, examined at BNL in 1969, show anomalously high ductilities, in that all seven specimens tested had total a elongation of 20-21.4%, which is greater than that specified for the unirradiated materials in the T-6 condition. There is no definitive explanation for this observation; the tensile strengths of these specimens are not abnormally low, so that radiation softening of the type observed after proton bombardment by Singh et al (7), does not appear to be a major factor here. (The age of the data makes this verification of this result impossible at the present time). Perhaps a radiation-induced over aging occurs initially, or the CRDF inadvertently was overheated (by γ -heating) following its removal from the HFBR (or it was not type 6061-T6 originally). Assuming the result is a real observation, we have chosen to draw our trend curves through this point, which tends to accentuate the subsequent loss in ductility at higher fluences. This observation does not affect our conclusion that embrittlement appears to saturate at approximately 9% above a thermal fluence of $1.8 \times 10^{23} \text{n/cm}^2$ in the HFBR. Admittedly, this conclusion is based on only two sets of data, taken 7 years apart; additional data will be obtained in 1989 when the next CRDF specimens will be removed for surveillance.

Finally, the role of the fast neutron fluence on these phenomena needs to be discussed. The relatively low tensile strengths and high ductilities of the specimens from the high-fast flux end of the V-13 shroud, compared to the trend of the CRDF data, (Figure 8) suggest that a high fast fluence may have the beneficial effect of randomizing the locations of the Si atoms (these fluences are well above 1 dpa) and therefore reducing their effects on mechanical properties of the alloy.

Microstructures of these specimens have not been studied due to lack of funding. It is planned to examine specimens from the next CRDF scheduled for removal in 1989.

CONCLUSIONS

1. The principal radiation effects on 6061-T6 Al at 333°K appear to arise from thermal neutrons, which transmute Al to Si.
2. Radiation effects appear to be saturating above $1.8 \times 10^{23} \text{n/cm}^2$ thermal.
3. HFBR beam tube tips have adequate ductility for continued operation.
4. It is impossible to establish a "cut-off" point based on the available radiation effects data.

LIST OF TABLES AND FIGURES

Table 1 - Summary of Data on HFBR Irradiation of Al-6061-T6

Table 2 - Tensile, Fluence and Silicon Data on V-15 Flow Shroud Removed After 179,556 MWD

Table 3 - Tensile, Fluence and Silicon Data on Control Rod Follower A-8 Removed after 189,105 MWD

Figure 1 - Plan view of the location of the experimental beam tubes and irradiation facilities within the reactor vessel.

Figure 2 - Calculated neutron flux distribution as a function of radial distance from the center of the core.

Figure 3 - Fluence dependence of tensile properties of 6061-T6 at 323K (4).

Figure 4 - Sketch of in-core flow shroud showing location of tensile specimens and ID number corresponding to Table 2.

Figure 5 - Sketch of control rod follower showing location of tensile specimens and ID numbers corresponding to Table 3. Follower is 2.5 cm pipe, 3mm thick.

Figure 6 - Effect of fast ($E > 0.1$ MeV) fluence on the tensile strength of aluminum alloy 6061-T6, HFBR Data

Figure 7 - Effect of fast ($E > 0.1$ MeV) fluence on the ductility of aluminum alloy 6061-T6, HFBR data.

Figure 8 - Effect of thermal fluence on tensile strength of aluminum alloy 6061-T6 HFBR data

Figure 9 - Effect of thermal fluence on ductility of aluminum alloy 6061-T6 HFBR data

Figure 10 - Comparison between HFBR tensile strength data and HFIR and Petten results

Figure 11 - Effect of thermal neutron radiation on the ductility of aluminum alloys

REFERENCES

1. BNL 24182 Revised, HFBR Handbook, August, 1983.
2. Graber, M. J. and Ronsick, J. H., IDO-16628, "ETR Radiation Damage Surveillance Programs, Progress Report 1," 1/27/61.
3. Farrell, K. and Richt, A. E., "Microstructure and Tensile Properties of Heavily Irradiated 1100-O Aluminum," Effects of Radiation on Structural Materials, ASTM STP 683, J. A. Sprague and D. Kramer, Eds., American Society for Testing and Materials, 1979, pp. 427-439.
4. Farrell, K. and King, R. T., "Tensile Properties of Neutron-Irradiated 6061 Aluminum Alloy in Annealed and Precipitation-Hardened Conditions," Effects of Radiation on Structural Materials, ASTM STP 683, J. A. Sprague and D. Kramer, Eds., American Society for Testing and Materials, 1979, pp. 440-449.
5. Farrell, K., "Radiation Response of Aluminum and its Alloys after Exposure in the High Flux Isotope Reactor - Paper presented at AIME Annual Meeting, Chicago, March, 1981.
6. Lijbrink, E., Grol, H. J. van, Dekker, F. and Witzenburg, W. van, "Effects of Neutron Irradiation on the Mechanical Properties of a 5154-O Type Aluminum Alloy," Effects of Radiation on Materials: Eleventh Conference, ASTM STP 782, H. R. Brager and J. S. Perrin, Eds., American Society for Testing and Materials, 1982, pp. 765-778.
7. Singh, B.N., Lohmann, W. Ribbens, A., and Sommer, W.F. "Microstructural Changes in Commercial Aluminum Alloys Caused by Irradiation with 800-MeV Protons," Radiation-Induced Changes in Microstructure: 13th International Symposium (Part I), ASTM STP 955, F.A. Garner, N.H. Packan, and A.S. Kumar, Eds., American Society for Testing and Materials, Philadelphia, 1987, pp. 508-519.

Table 1

Summary of Data on HFBR Irradiation of Al-6061-T6

Source	Fluence, n/cm ²		Tensile strength ksi	% Elongation (total)	# of Specimens
	E > 0.1 MeV	Thermal			
Alcoa Handbook	0	0	45	17	-
Chow & Jones	0	0	48.4 \pm 2.0	17.5 \pm 2.5	2
ORNL	0	0	50.8 \pm 0.6	11.0 \pm 1	3
Czajkowski	0	0	47.8 \pm 1	10.3 \pm 0.5	4
Surveillance	5 \times 10 ¹⁹	2.7 \times 10 ²⁰	48.2 \pm 1.8	15 \pm 1.0	2
Surveillance	2 \times 10 ²⁰	1.07 \times 10 ²¹	50.4 \pm 0.4	17.0	2
Surveillance	1.2 \times 10 ²¹	6.4 \times 10 ²¹	61.0 \pm 3.0	12	2
CRDF A-6	7.9 \times 10 ²¹	1.7 \times 10 ²³	82.7 \pm 2.3	8.2 \pm 1.6	4
CRDF A-7	2.2 \times 10 ²¹	4.9 \times 10 ²²	62.3 \pm 1.8	20.7 \pm 0.7	7 ^Δ
CRDF A-8	1.5 \times 10 ²²	3.2 \times 10 ²³	86.5 \pm 8	8.6 \pm 2	6
(A-8, ignoring lowest sample #)			(88.3 \pm 2.8)	(9.0 \pm 0.3)	(5)
V-15,13" *	1.9 \times 10 ²²	1.5 \times 10 ²³	71.6 \pm 1.2	10.2 \pm 0.7	2
V-15,17" *	9.3 \times 10 ²²	1.2 \times 10 ²³	62.0 \pm 0.4	11.6 \pm 1.4	2
V-15,23" *	1.6 \times 10 ²³	9.2 \times 10 ²²	50.8 \pm 2	12.9 \pm 1.1	2
V-15,28" *	1.9 \times 10 ²³	1.0 \times 10 ²³	55.2 \pm 0.8	15.7 \pm 1.9	2

Δ Chow and Jones also include data from four specimens from the upper end of the tube, which contained little induced activity, indicating a much lower thermal fluence. These data were omitted from this evaluation.

* inches from top of vertical thimble flow shroud.

† The same specimen gave low values of both T.S. and % elongation.

Table 2 Tensile, Fluence and Silicon Data on V-15 Flow Shroud removed after 179,556 MWD.

Specimen ID No.	Tensile Strength, psi	% Elongation	% Si Increase	Thermal Fluence, n/cm ² (from Si)
1	70,400	9.5	3.18	1.66×10^{23}
1a	72,800	10.9		
2	61,600	10.25	*	*
2a	62,400	13.0		
3	48,000	11.8		
3a	52,800	12.6	0.95	4.9×10^{22}
3b	49,600	13.2		
3c	52,800	14.0		
4	56,000	17.6	1.26	6.5×10^{22}
4a	54,400	13.75		
5	48,000	9.75	unirradiated specimen	
6	46,400	10.13	unirradiated specimen	
7	48,000	10.44	unirradiated specimen	
8	48,800	10.88	unirradiated specimen	

NOTES:

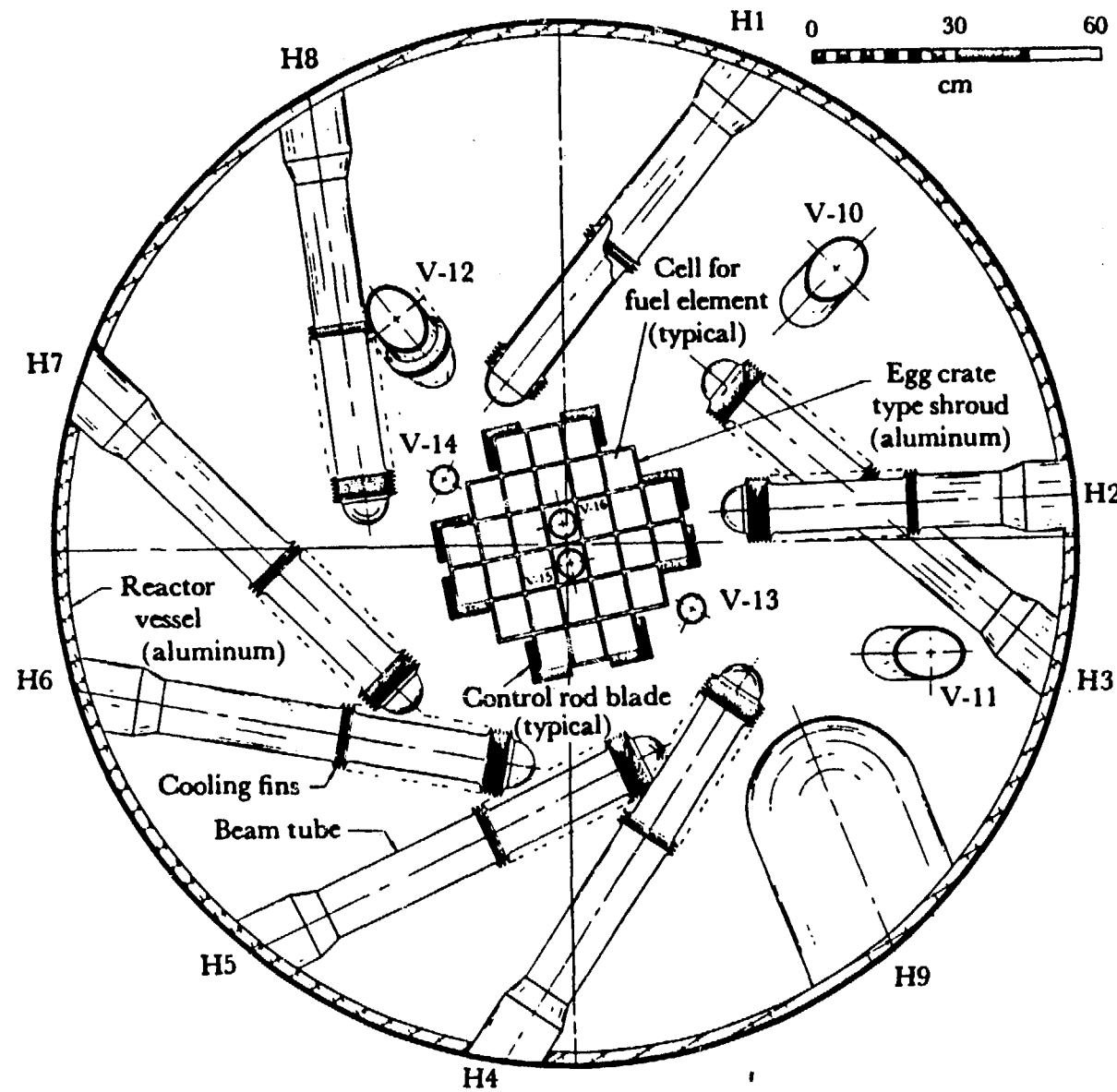
1. See Fig. 5 for location of specimens.
2. One silicon analysis performed for each group of specimens except for asterisked group of specimens (ID #2) where sample was lost.
3. A 0.6% Si content is assumed for the unirradiated material.
4. Fluences shown inferred from silicon measurements. Fluences calculated from fresh core flux distribution range from $1-1.5 \times 10^{23}$ n/cm².

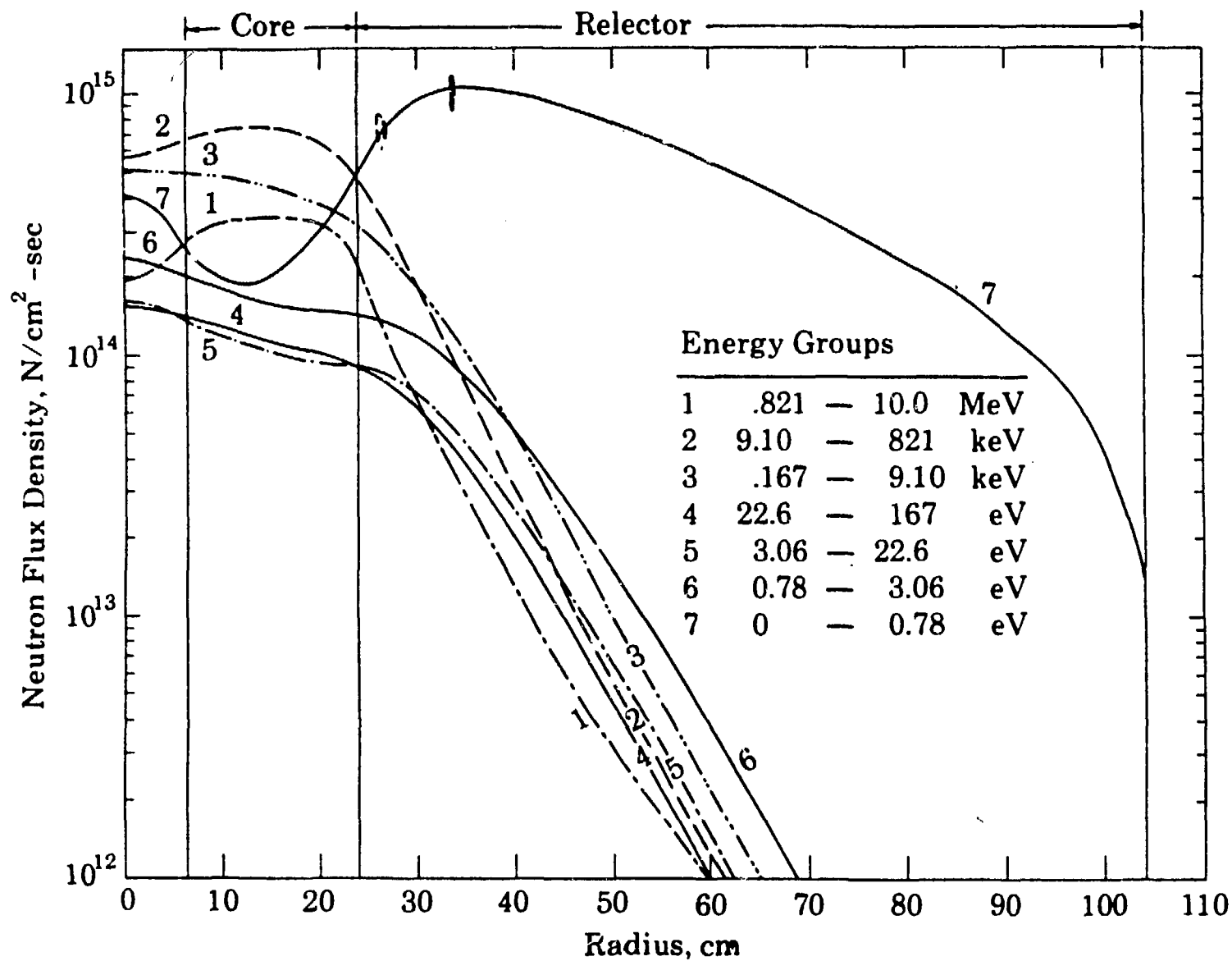
Table -3 Tensile, Fluence and Silicon Data on Control Rod Follower A-8 removed after 189,105 MWD.

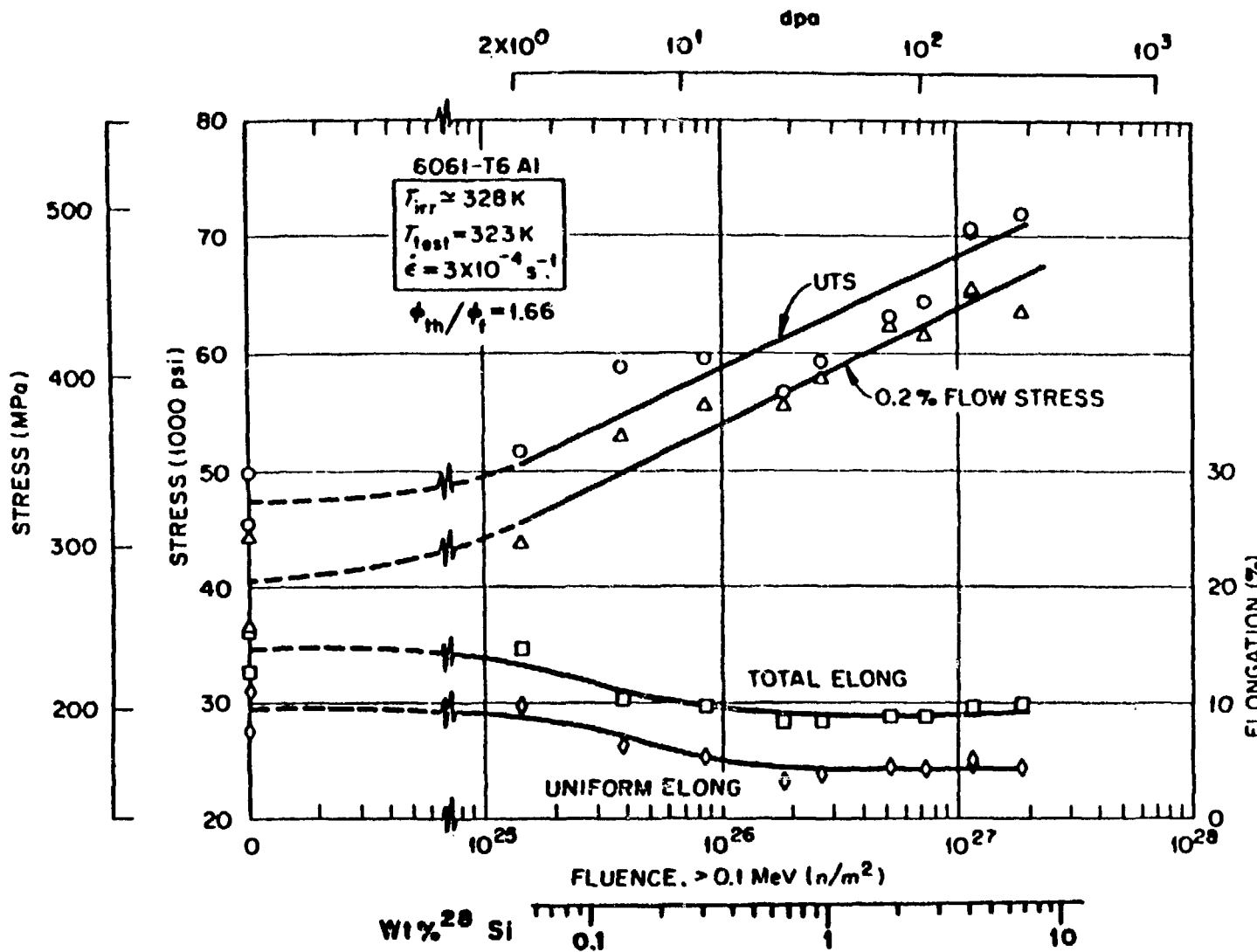
<u>Specimen ID No.</u>	<u>Tensile Strength, psi</u>	<u>% Elongation</u>	<u>% Si Increase</u>	<u>Thermal Fluence, n/cm²(from Si)</u>
1	87,900	9.4	6.11	3.23×10^{23}
2	89,100	8.75		
3	87,900	7.75	6.03	3.19×10^{23}
4	91,000	9.5		
5	78,000	6.6	3.31	1.73×10^{23}
6	85,400	9.25		

NOTE:

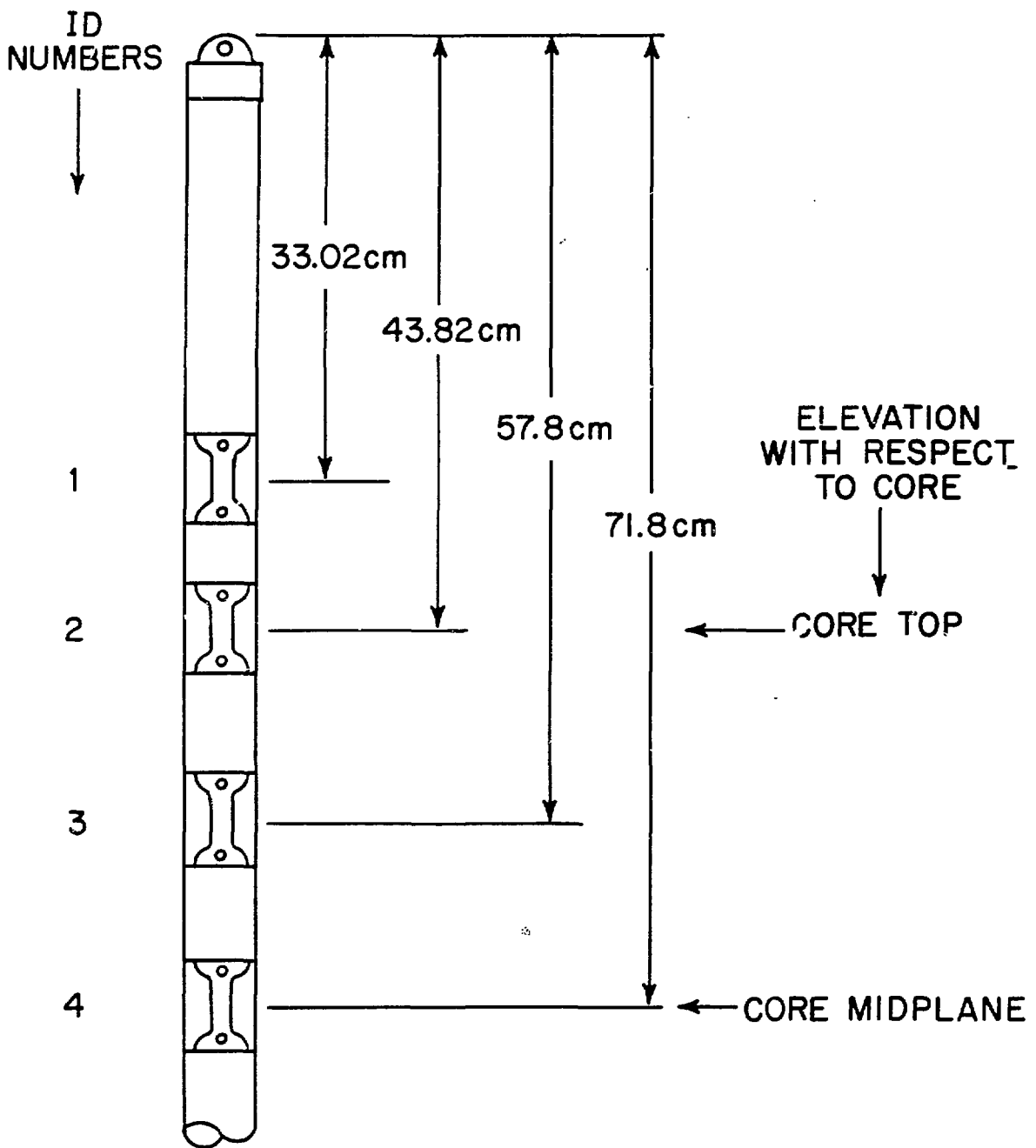
1. See Figure 4 for location of specimens.
2. One silicon analysis performed for each pair of tensile specimens.
3. A 0.6% Si content is assumed for the unirradiated material.
4. Fluences shown are inferred from silicon measurements. Maximum thermal fluence calculated from fresh core flux distribution in follower is 3.2×10^{23} n/cm².

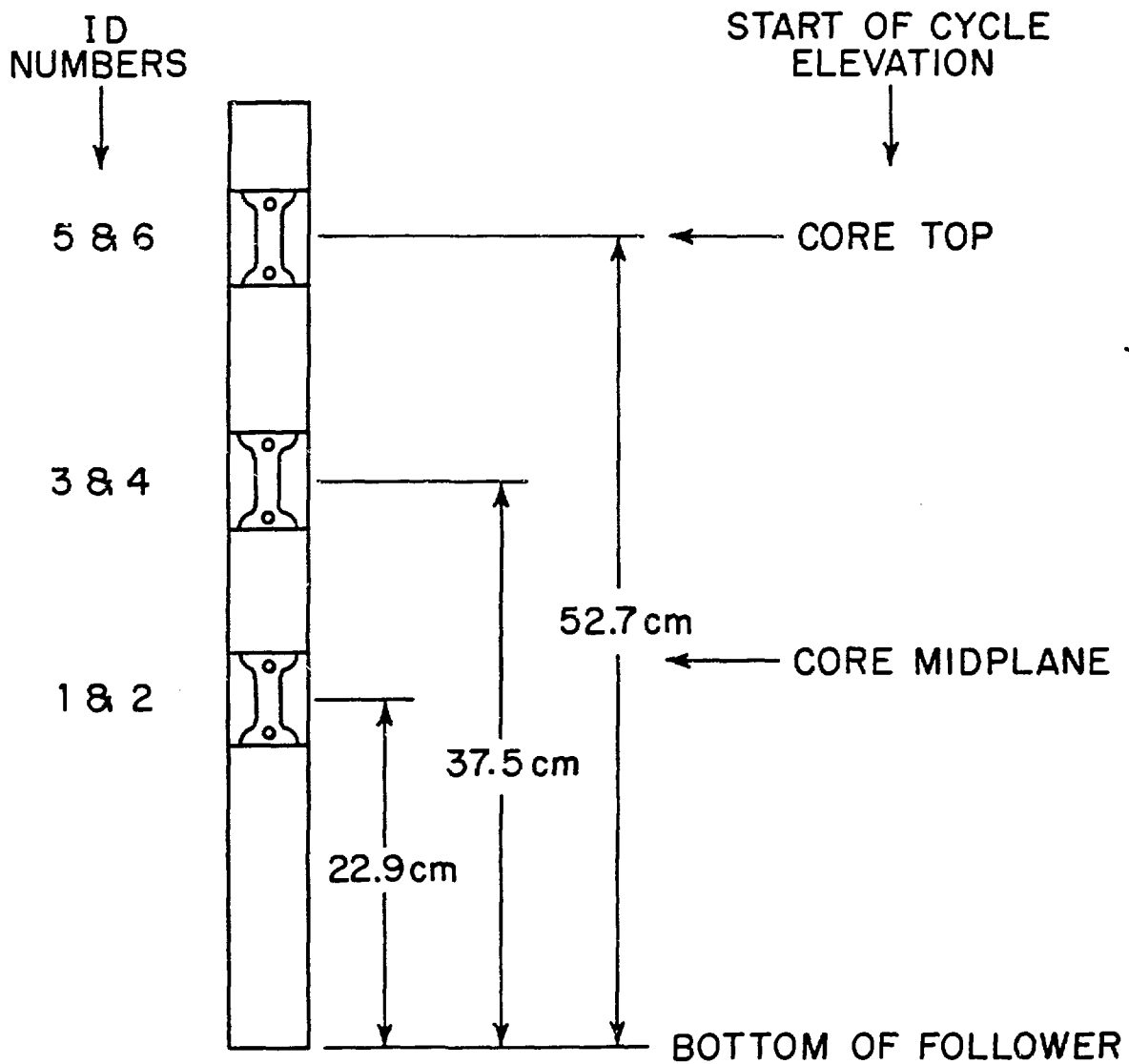


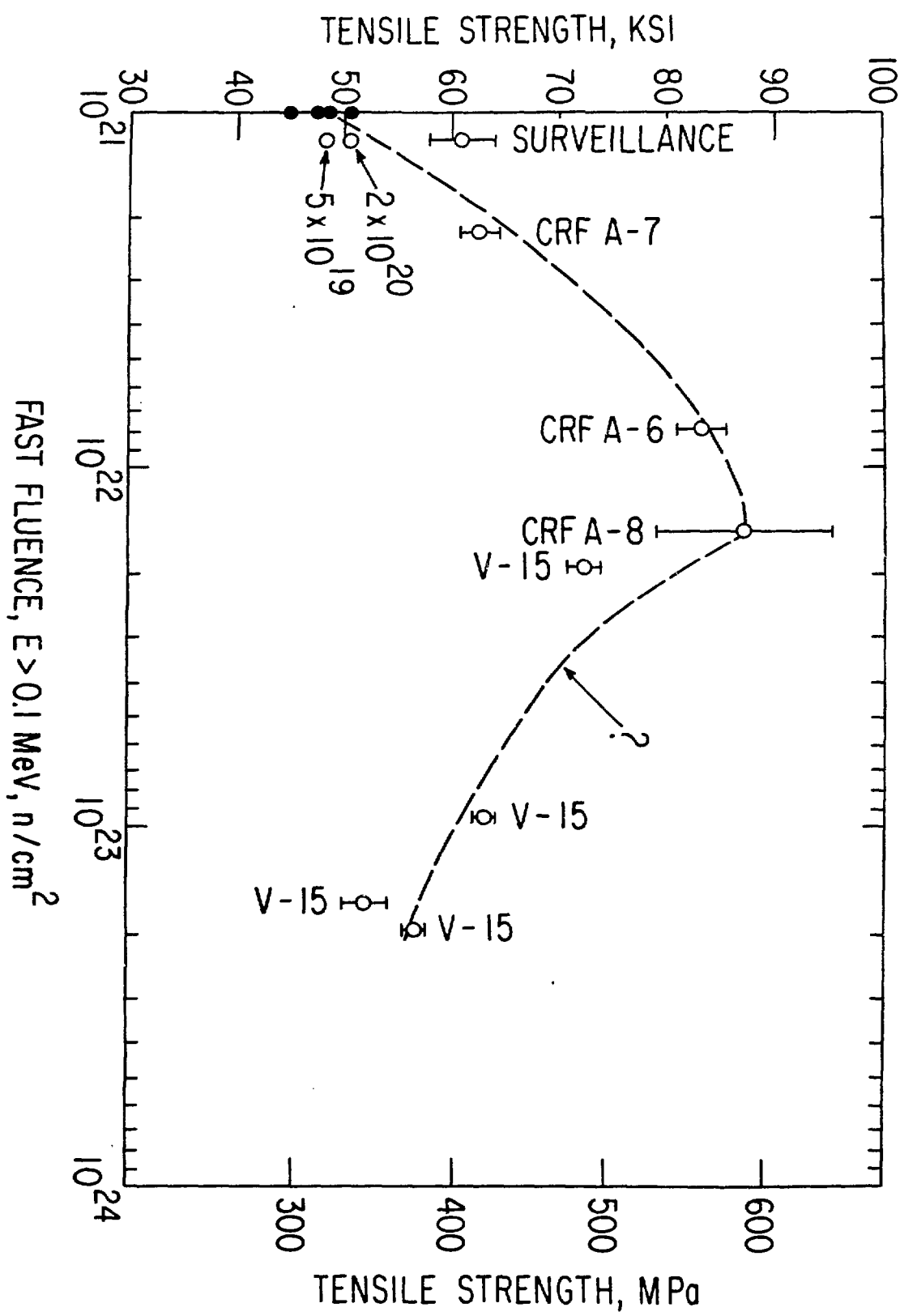


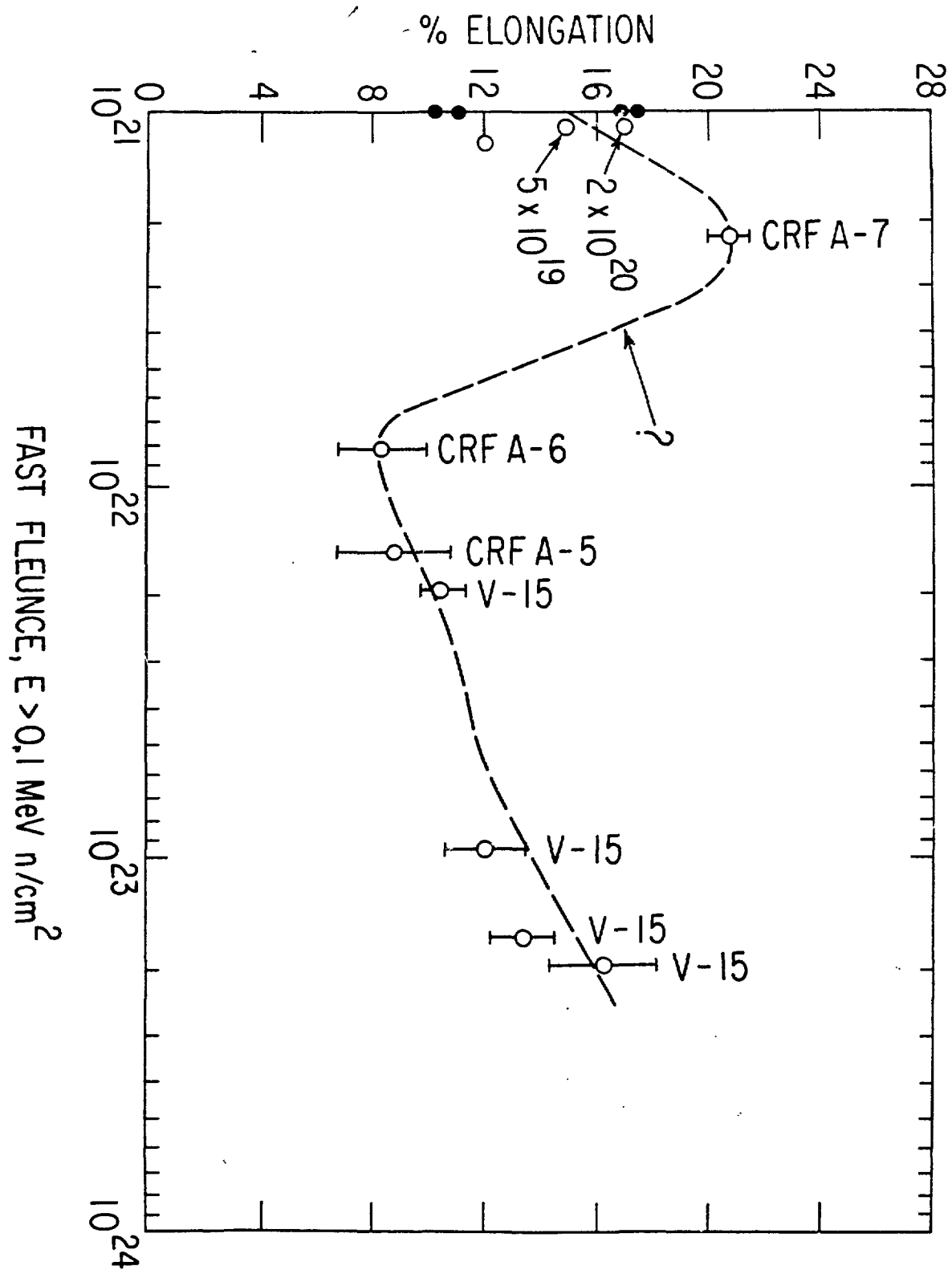


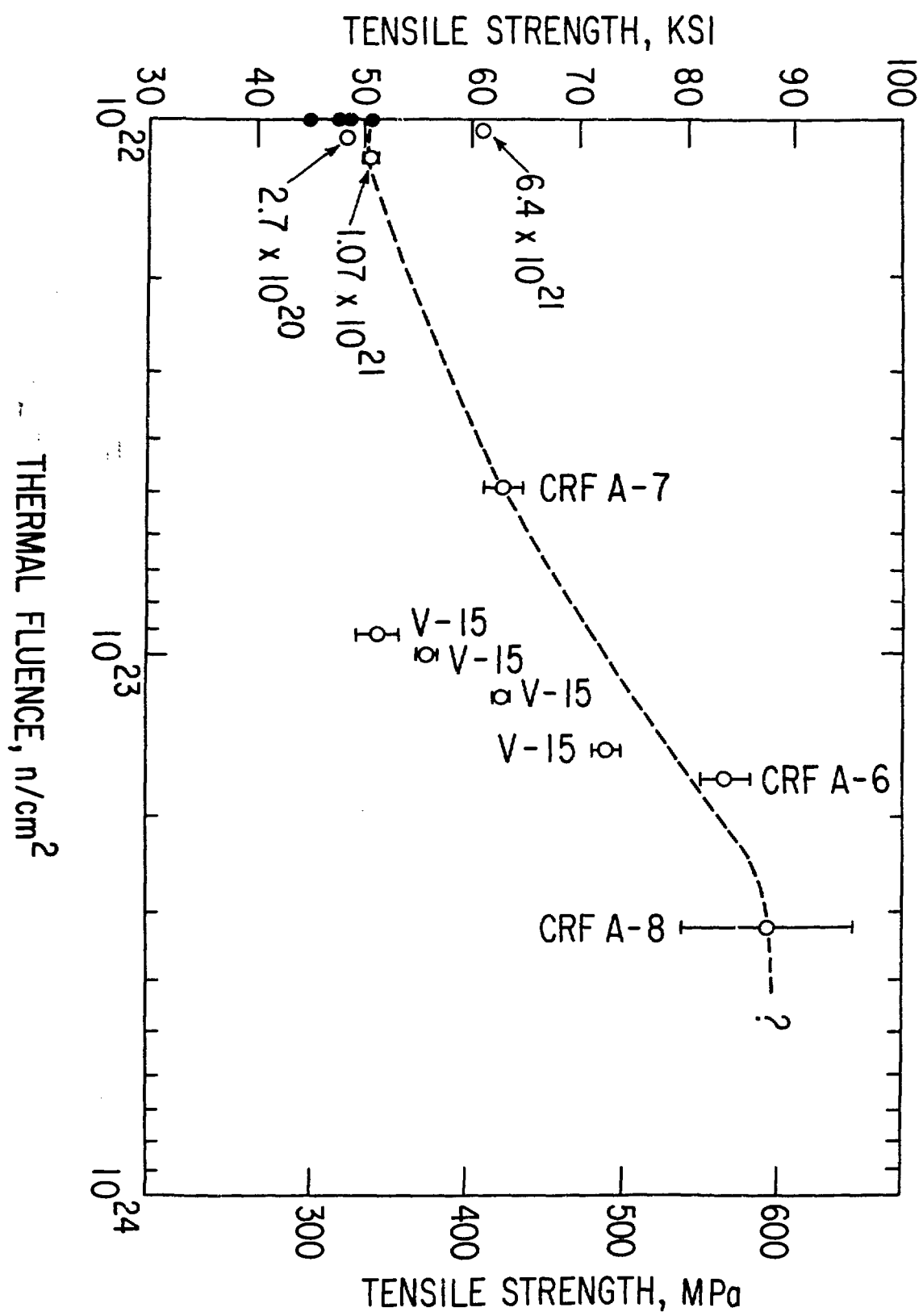
—Fluence dependence of tensile properties of 6061-T6 at 323 K.

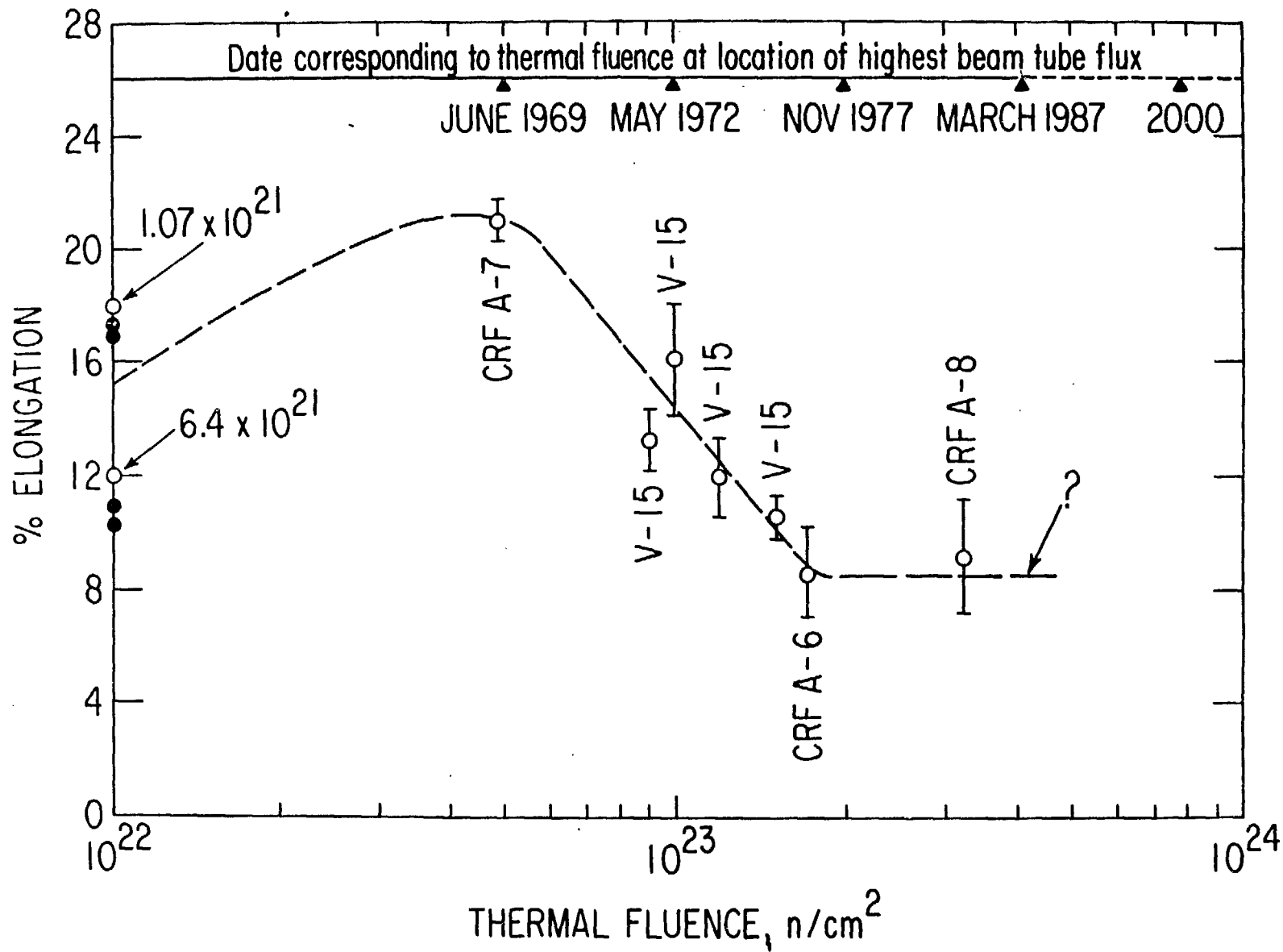


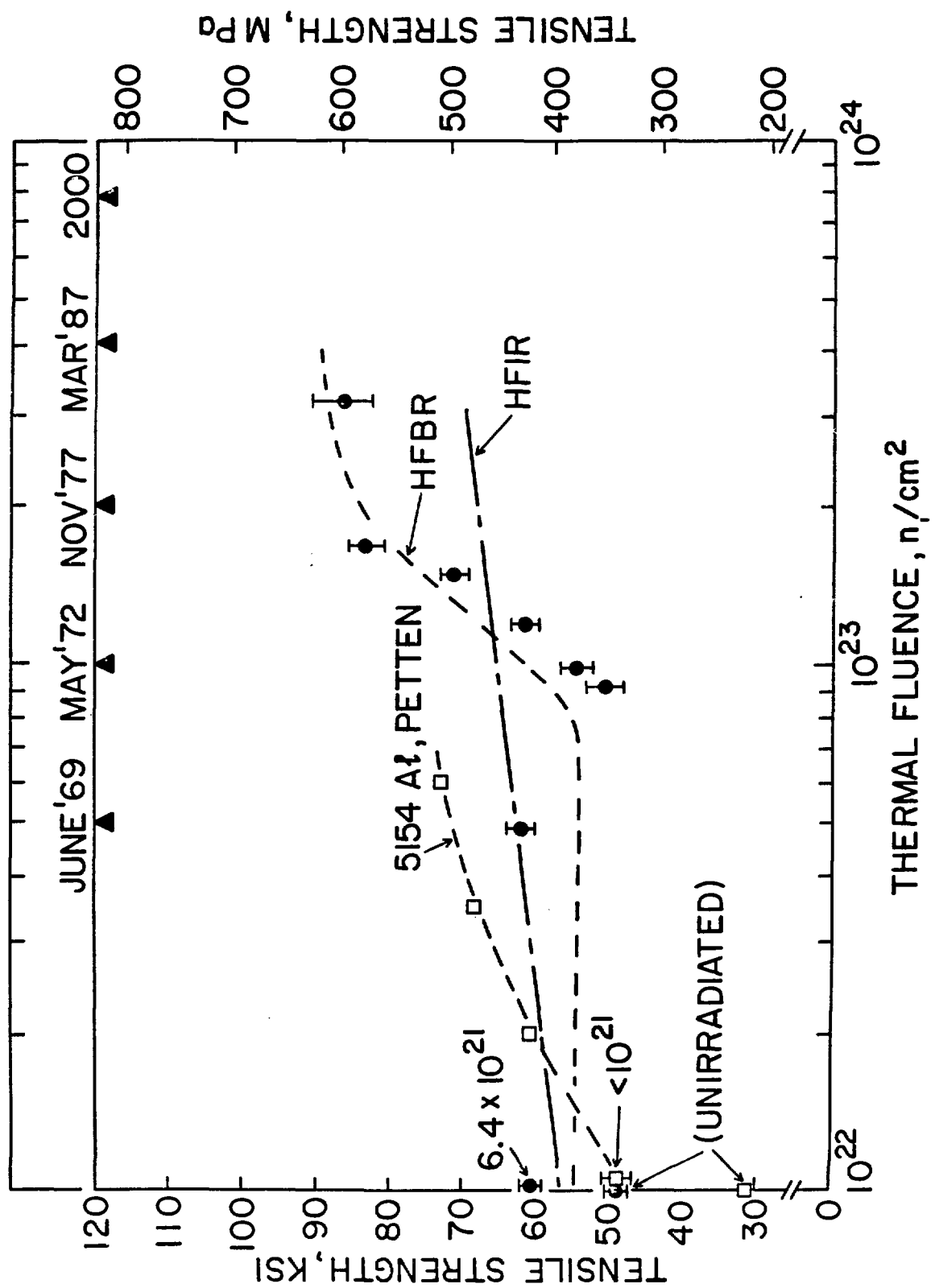












INCREASE IN SILICON CONTENT, wt. %

2

5

10

12.6

